- 1 Effects of Mixing State on Water-Uptake Properties of
- 2 Ammonium Sulfate Organic Mixtures
- 3 Patricia N. Razafindrambinina¹, Kotiba A. Malek², Kristin DiMonte³, Joseph Nelson Dawson³,
- 4 Timothy M. Raymond⁵, Dabrina D Dutcher^{5,6}, Miriam Arak Freedman^{3,4}, and Akua A. Asa-
- 5 Awuku^{1,2}
- 6 ¹Department of Chemistry and Biochemistry, University of Maryland, College Park, MD 20742,
- 7 United States
- 8 ²Department of Chemical and Biomolecular Engineering, University of Maryland, College Park,
- 9 MD 20742, United States
- ³Department of Chemistry, The Pennsylvania State University, University Park, PA 16802, United
- 11 States

- 12 ⁴ Department of Meteorology and Atmospheric Science, The Pennsylvania State University,
- 13 University Park, PA 16802, United States
- ⁵Department of Chemical Engineering, Bucknell University, Lewisburg, PA 17837, United States
- 15 ⁶Department of Chemistry, Bucknell University, Lewisburg, PA 17837, United States
- 17 Correspondence to: Akua Asa-Awuku (asaawuku@umd.edu); Miriam Arak Freedman
- 18 (maf43@psu.edu); Dabrina D Dutcher (ddd014@bucknell.edu); Timothy M. Raymond
- 19 (traymond@bucknell.edu).

- 20 Keywords: hygroscopicity, water-soluble, organic aerosol, cloud condensation nuclei, sucrose,
- 21 levoglucosan

ABSTRACT

23

24

25

26

27

28

29

30

31

32

33

34

35

36

37

38

39

Aerosol particles in the atmosphere have the ability to uptake water and form droplets. The droplets formed can interact with solar radiation (indirect effect of aerosols) and influence the net radiative forcing. However, the magnitude of change in radiative forcing due to the indirect effect of aerosols remains uncertain due to the high variance in aerosol composition and mixing states, both spatial and temporally. As such, there is a need to measure the water-uptake of different aerosol particle groups under controlled conditions to gain insight into the wateruptake of complex ambient systems. In this work, the water-uptake (hygroscopicity) of internally and externally mixed ammonium sulfate – organic binary mixtures were directly measured via three methods and compared to droplet growth prediction models. We found that subsaturated water-uptake of ammonium sulfate-organic mixtures agreed with their supersaturated hygroscopicities, and mixing state information was able to be retrieved at both humidity regimes. In addition, we found that solubility-adjusted models may not be able to capture the water-uptake of viscous particles, and for soluble organic aerosol particles, bulk solubility may not be comparable to their solubility in a droplet. This work highlights the importance of using multiple complementary water-uptake measurement instruments to get a clearer picture of mixed aerosol particle hygroscopicity, especially for increasingly complex systems.

40

41

43

44

45

- Synopsis Statement: This work provides water-uptake measurements of mixed aerosol particles
- 42 that are prevalent in the atmosphere that can be useful in improving climate models.

INTRODUCTION

Aerosol particles in the atmosphere can indirectly affect the radiative budgets through droplet and cloud formation (Haywood and Boucher 2000). Clouds and droplets can reflect or

absorb solar radiation, leading to a cooling or warming effect on the atmosphere and Earth's surface (Lohmann and Feichter 2005). Changes in aerosol particles' water-uptake properties (hygroscopicity) have significant effects on air quality, climate, and visibility as it can lead to changes in their optical properties and can also modify their contribution towards the net radiative forcing (Lohmann and Feichter 2005). Additionally, the indirect effect of aerosols is the largest source of uncertainty in climate and radiative forcing modeling, partly due to the wide variety of composition of atmospheric aerosols that can evolve spatially and temporally (IPCC 2021).

Inorganic and organic particles are found in the atmosphere and can form clouds and droplets. The water-uptake properties of inorganic particles have been well characterized, and the water-uptake properties of organic aerosols have been extensively studied (Dawson et al. 2020; Altaf et al. 2018; Zhang et al. 2016; Lei et al. 2014a; Jimenez et al. 2009; Prenni et al. 2001, 2007; Kanakidou et al. 2005; VanReken et al. 2005; Raymond and Pandis 2003; Cruz and Pandis 1998). However, ambient aerosols often exist as a mixture of organic and inorganic particles, and models have shown that the presence of organic particles in mixed aerosols can significantly affect particle growth and water-uptake (Nandy et al. 2021); and as such, research into the water-uptake of mixed aerosol particles under controlled conditions is important to further our understanding of the water-uptake of atmospheric aerosol particles.

The mixing states of aerosol particles can be classified into externally or internally mixed. An external mixture occurs when different aerosol species can be assumed to be physically separated from each other. For example, for binary external mixtures, two distinct populations would be observed. Internally mixed (homogenous or phase separated) aerosols consist of particles with the same mixture of chemical species (Riemer et al. 2019; Altaf et al. 2018). Changes in the water-uptake of mixed particles, at both sub- and supersaturated conditions, have been the focal

point of several studies. Cruz and Pandis (2000) reported that an increase in organic fraction reduced the growth factor (*G_f*) of mixed particles (Cruz and Pandis 2000). Additionally, Brooks et al. (2002) found that the presence of water-soluble dicarboxylic acids can lower the deliquescence relative humidity (DRH) of ammonium sulfate, and that less-soluble dicarboxylic acids did not affect the DRH of the inorganic (Brooks et al. 2002). Furthermore, Bilde et al. (2004) suggested that small amounts of salt can significantly affect the water-uptake of mixed particles (Bilde and Svenningsson 2004). Lei et al. also demonstrated that the presence of a hygroscopic organic such as levoglucosan decreased the apparent DRH of ammonium sulfate, whereas the presence of a non-hygroscopic organic compound such as 4-Hydroxybenzoic acid reduced the water-uptake of mixed particles. The results of Lei et al. suggest that the presence of hygroscopic organic particles may be the primary reason that causes an enhancement in water-uptake of mixed particles compared to pure inorganics when RH < DRH (Lei et al. 2014b).

Supersaturated water-uptake of mixed (ammonium sulfate and organic acids) particles has been investigated by Abbatt et al. using a continuous flow, thermal-gradient diffusion chamber. It was demonstrated that the presence of water-soluble species in the particle lowers the vapor-pressure and energy barrier needed for droplet formation. Additionally, Abbatt et al. showed the additive nature of the vapor-pressure-lowering effect for binary mixtures (Abbatt et al. 2005). Water-uptake was parameterized as droplet activation diameters, and it was reported that for soluble organics, hygroscopicity of the mixed aerosol particles can be predicted using a simple Köhler theory model that assumes complete solubility with the droplet having the surface tension of pure water. However, when organics are less soluble, the consideration of limited solubility was determined to be important. For example, thick organic coatings around an inorganic core can lead to a complete deactivation of ultrafine ammonium sulfate particles (< 120 nm) (Abbatt et al. 2005).

For sparingly soluble and non-hygroscopic species such as adipic acid, Broekhuizen et al. (2004) showed that the presence of a small fraction of a soluble salt can greatly reduce the activation diameter of internally mixed adipic acid – ammonium sulfate particles, and that it can be predicted well by Köhler theory (Broekhuizen et al. 2004).

For externally mixed particles, Schill et al. showed that it is possible for the supersaturated water-uptake of each pure component to be differentiated in the measured particle activation curves, however their hygroscopicities must have a big enough difference (Schill et al. 2015). For a binary mixture of compounds with similar hygroscopicities, the activation curves do not clearly indicate the number of pure compounds. In contrast, a binary mixture of a highly hygroscopic and a sparingly hygroscopic species led to multiple sigmoid fittings, with each inflection point indicating the presence of a different species (Vu et al. 2019; Schill et al. 2015).

Much of the literature on the water-uptake of mixed aerosols focuses on the chemical and physical properties of the mixtures and their effect on particle hygroscopicity (Vu et al. 2019; Jing et al. 2016; Liu et al. 2016; Lei et al. 2014b; Padró et al. 2012). Few studies have used multiple instruments to measure, describe, and analyze water-uptake at both subsaturated and supersaturated conditions (Xu et al. 2021; Wex et al. 2009; Svenningsson et al. 2006). Fewer still have evaluated the performance of different hygroscopicity measurement instruments to capture the water-uptake of various systems (Dawson et al. 2020; Rickards et al. 2013; Zardini et al. 2008). For example, Dawson et al. (2020) measured the water-uptake of pure water-soluble organic compounds using a CCNC, HTDMA, and cavity ring-down spectroscopy (CRDS) and found that for pure water-soluble compounds, the three instruments were in agreement (Dawson et al. 2020). However, little is known about the comparison of water-uptake instruments for mixed aerosol compositions.

Intercomparison of measured water-uptake across different instruments and systems can be done by first converting the directly measured parameters such as, activation diameters and growth factors, into a single hygroscopicity parameter, (κ). κ is a valuable tool for comparison, as theoretically, it is a composition-dependent parameter and conceptually varies little between suband supersaturated conditions (Petters and Kreidenweis 2007, 2008, 2013). Additionally, κ can be used with the Zdanovskii-Stokes-Robinson (ZSR) mixing rule, which assumes volume additivity and that each species independently uptakes water, to predict the hygroscopicity of a mixed system (Petters and Kreidenweis 2007; Svenningsson et al. 2006).

115

116

117

118

119

120

121

122

123

124

125

126

127

128

129

130

131

132

133

134

135

136

137

In this work, we measured the water-uptake of internal and external mixtures of the atmospherically prevalent salt, ammonium sulfate, with three organic compounds (Lei et al. 2014a; Pashynska et al. 2002). The organic compounds used are adipic acid, which is a dicarboxylic acid known to be emitted from biomass burning and motor exhaust, and two sugars: levoglucosan and sucrose, both of which are tracers for biomass burning (Marynowski and Simoneit 2022; Hays et al. 2002; Kaplan and Kawamura 1987). We applied three distinct experimental droplet growth methods to measure the hygroscopicity of binary ammonium sulfate – organic mixtures. The instrumentation has been previously described by Dawson et al. (2020), however the usage and advantages of such suite of instruments have yet to be evaluated for mixed particles. The three organics used in this work are levoglucosan, sucrose, and adipic acid, all of which are prevalent in the atmosphere and have been extensively studied, and all of which are biomass burning byproducts (Ott et al. 2020; Jing et al. 2016; Liu et al. 2016; Lei et al. 2014a; Rickards et al. 2013; Yttri et al. 2007; Rosenørn et al. 2006; Broekhuizen et al. 2004; Marcolli et al. 2004; Pashynska et al. 2002; Cruz and Pandis 1998). To our knowledge, this is the first work to evaluate and compare measured binary (internally and externally mixed) aerosol particle water-uptake by CCNC, HTDMA, and CRDS to identify advantages and disadvantages of each instrument towards the estimation of the perceived single-parameter hygroscopicity, κ . Furthermore, we explore the use of Kohler theory and Zdanovskii-Stokes-Robinson (ZSR) models to predict experimental measurements. A layer of complexity is added to this work through the evaluation of two κ retrieval methods from optical measurements of mixed aerosols that have only been applied in few other studies (Razafindrambinina et al. 2022; Dawson et al. 2020; Kreidenweis and Asa-Awuku 2014a).

MATERIALS AND METHODS

Sample Preparation

As previously mentioned, the three organics selected for this study are relevant and abundant in the atmosphere. However, they were also selected due to their range of atomic oxygen to carbon ratio (O:C), molecular weight, and solubility they provide, which may lend insight into κ variations (Table 1). Levoglucosan (99%, ACROS Organics) had the highest density and theoretical κ (κ_{theory}), sucrose (99% Fisher Chemical) had the highest solubility and O:C, and adipic acid (99%, Sigma Aldrich).

Table 1. Physical properties of organic compound, and calculated theoretical κ -values assuming infinite and limited solubility.

Organic Compound	Molecular Weight [g mol ⁻¹]	Solubility @ 298 K [g L ⁻¹]	Density [g mL ⁻¹]	O:C	κ _{theory} (ideal)	κ_{theory} (limited solubility)
Levoglucosan	162.1	62.3 ^a	1.7 ^b	0.83	0.19	0.02
Sucrose	342.3	2040°	1.59°	0.92	0.08	0.08
Adipic Acid	146.1	24 ^d	1.36 ^e	0.67	0.17	0

^aThe Human Metabolome Database. http://www.hmdb.ca/ (accessed October 9, 2019)

^bValue predicted by ACS/Labs Percepta Platform? PhysChem Module

^cRumble, J. R.; Lide, D. R.; Bruno, T. J. CRC handbook of chemistry and physics: a ready-reference book of chemical and physical data, 2017

dMITI (Ministry of International Trade and Industry) (1992). Biodegradation and Bioaccumulation Data of Existing
 Chemicals Based on the Chemical Substances Control Law (CSCL).

^eHaynes, W.M. (ed.). CRC Handbook of Chemistry and Physics. 95th Edition. CRC Press LLC, Boca Raton: FL 2014-2015, p. 3-10

Samples were prepared by dissolving 50 mg of solute in 400 ml of UltraPure water (high-performance liquid chromatography grade or Millipore(R) water >18 M Ω). Internally mixed samples were prepared by dissolving 50 mg total solids with 5, 25, 50, 75, and 95 wt % of the organic compound in 400 ml of water. For external mixtures, two separate solutions (0.125 mg/ml) were prepared for ammonium sulfate and the organic compound. The composition of the external mixtures were controlled by valves downstream of each of the atomizers. Prior to HTDMA measurements, each component of the mixture was atomized, dried, and the particle mass concentration ($\mu g \ m^{-3}$) of the organic and ammonium sulfate was measured by a DMA in scanning mode. Valves were then adjusted to achieve target organic mass fraction (between 0.05 and 0.95). Polydisperse aerosols were created using a constant output atomizer (TSI 3076). Particles were then dried via two diffusion dryers arranged in series upstream of the three water-uptake measurement instruments: a cloud condensation nuclei counter (CCNC), a humidified tandem differential mobility analyzer, and a cavity ring-down spectrometer (Fig. 1)

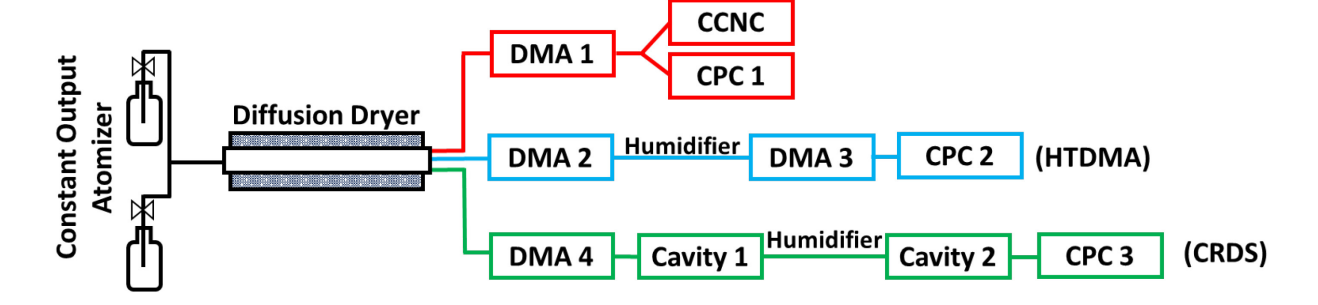


Figure 1. Schematic of the three different experimental setups. For each measurement method, setup was modified to the CCNC (red), HTDMA (blue), or CRDS (green) configuration.

Intercomparisons of the hygroscopicities of ammonium sulfate-organic binary mixtures were done by retrieving κ from the measured parameters (critical activation diameters, D_{p50}), geometric growth factor (G_f), and optical growth factors (fRH)) as detailed below.

Cloud Condensation Nuclei Activity Measurements

The dry, polydisperse aerosol stream was first size selected by a differential mobility analyzer (DMA 1; TSI DMA 3081L) in scanning mode to create a stream of monodisperse aerosol particles. Downstream of electrical mobility selection, the sample flow was split and then sampled into the CCNC (DMT CCN-100, sample flow = 0.5 L min⁻¹) and condensation particle counter (CPC; TSI 3775, sample flow = 0.3 L min⁻¹). The CCNC counted the number of activated particles or cloud condensation nuclei (CCN) at a given supersaturation (in this work, the CCNC was operated at 0.4, 0.6, 0.8, and 1.0 % supersaturations), and the CPC provided the total number of particles (CN) at each size bin.

The CCNC method parameterizes water-uptake in terms of a particle's critical activation diameter (D_{p50}). The critical activation diameter is defined as the dry particle diameter at which 50% of the population activates into droplets. In this work, the Scanning Mobility CCN Analyzer (SMCA) software was used to obtain the ratio between CCN and CN and estimate D_{p50} . The SMCA applied a multiple charge correction and fits a sigmoid curve through the measured data to estimate D_{p50} (Moore and Nenes 2009). A sample output of a CCNC data activation curve and an SMCA sigmoid fit is presented in Figure 2.

Internal and externally mixed particles can be distinguished through the measured activation curves. For internally mixed particles, a one sigmoid fit is sufficient to capture the measured data, whereas, for external mixtures, the number of sigmoid fits needed is equal to the number of components available for water-uptake in the mixture. In this work, binary external

mixtures were presented as two sigmoid curves and were fit as such. As a result, internal mixtures give a single D_{p50} value, and binary external mixtures yield two critical activation diameters, one from each sigmoid (Fig. 2) (Vu et al. 2019; Schill et al. 2015).

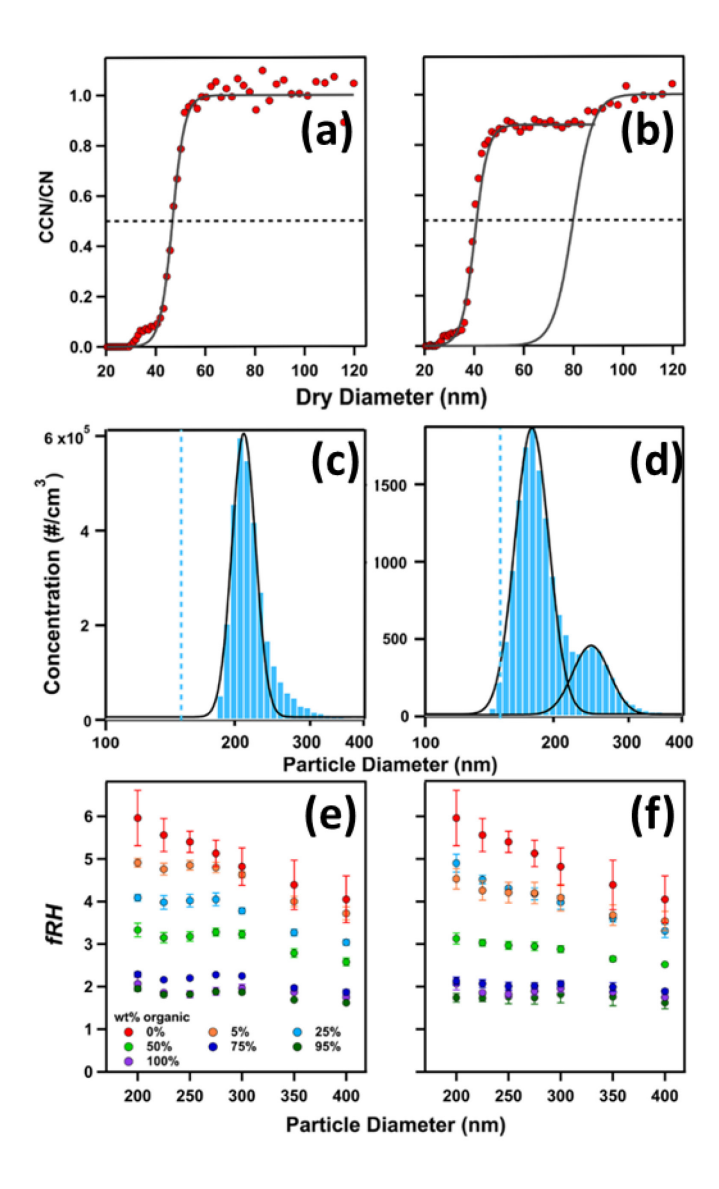


Figure 2 Example of measurement outputs from CCNC (a,b), HTDMA (c,d), and CRDS (e,f) for internal (left) and externally mixed (right) particles. Data fits are shown as solid black lines (sigmoid fit for a and b, lognormal fit for c and d). Dashed line in a and b represent 50% particle activation, and dashed blue line in c and d represent the selected particle size (in this example, 150 nm particles were selected.

Assuming that κ -values of each component of the mixtures are adequately differentiable (differences in water-uptake properties are detectable via the analysis software), the activation

curve of internal mixtures can be fit well with a single sigmoid (Fig. 2a), whereas external mixing can be identified by the presence of more than one sigmoid (Fig 2b). For binary external mixtures, two sigmoid curves are present: one curve represented ammonium sulfate, and the second (at larger diameters) represented the organic (Fig. 2) (Vu et al. 2019). Calibration of the CCNC was done prior to each experiment with ammonium sulfate aerosol, and the reported instrument supersaturation assumes a van't Hoff factor of 2.5 (Mikhailov and Vlasenko 2020; Rose et al. 2008)(Mikhailov and Vlasenko 2020; Rose et al. 2008). Hygroscopicity was then expressed in terms of the hygroscopicity parameter (κ_{CCNC}) through Equation 1 (Petters and Kreidenweis 2007).

222
$$\kappa_{CCNC} = \frac{4\left(\frac{4\sigma_{S/a}M_{W}}{RT\rho_{W}}\right)^{3}}{27D_{p50}^{3}\ln^{2}s}$$
 (1)

Where $\sigma_{s/a}$, $M_{\rm w}$, and ρ_w are the surface tension, molecular weight, and density of pure water, respectively. R and T are the gas constant and temperatures, and s is the calibrated instrument supersaturation.

Humidified Tandem Differential Mobility Analysis

A humidified tandem differential mobility analyzer (HTDMA) measured the subsaturated growth factor of binary mixtures. Aerosol particles with a dry mobility diameter (\underline{D}_{dry}) of 150, 250, and 350 nm were first size selected by an electrostatic classifier (DMA 2; TSI 3082) with an aerosol flowrate of 0.3 L min⁻¹ and sheath flow of 1.0 L min⁻¹. The size-selected particles were then humidified up to $80\% \pm 6\%$ RH with a Nafion humidification line (PermaPure M.H. series). Subsequently, the size distribution of humidified aerosol particles was measured by a second electrostatic classifier (DMA 3; TSI 3085) that has been humidified to 80% RH to prevent aerosol shrinkage, and the internal neutralizer was bypassed to prevent neutralization of already charged particles (Dawson et al. 2020).

For HTDMA experiments, κ was derived from the geometric growth factor (G_f). G_f is the ratio of the humidified particle diameter (D_{wet}) to its dry size (D_{dry}) and was calculated using Equation 2.

$$GF = \frac{D_{dry}}{D_{wet}}$$
 (2)

In the context of this work, D_{dry} corresponds to the selected particle size, and D_{wet} is the geometric mode of the probability density function fit of the wet distribution. For internal mixtures, a single wet distribution and growth factor is expected (Fig. 2c). In contrast, externally mixed aerosols would present as two wet distributions, and thus, two growth factor values (Fig. 2d).

Vapor pressure of water was assumed to approach that of a flat surface, and as such, the water activity can be approximated by RH. Thus, κ can be calculated via Equation 3 (Kreidenweis and Asa-Awuku 2014b; Petters and Kreidenweis 2007).

247
$$GF^3 = 1 + \kappa_{HTDMA} \left(\frac{\frac{RH}{100}}{1 - \left(\frac{RH}{100} \right)} \right)$$
 (3)

248 Cavity Ring-Down Spectroscopy

The cavity ring-down spectrometer has been previously described in detail (Dawson et al. 2020; Veghte and Freedman 2012; Freedman et al. 2009) and is only briefly described here. The generated aerosol particles at a flow rate of 1.5 L min⁻¹ are size selected using an electrostatic classifier (TSI 3080) and a Differential Mobility Analyzer (DMA 4; TSI 3081L) at a sheath flow rate of 15 L min⁻¹. After the particles are size selected, they enter the cavity ring down spectrometer, where their optical properties are measured at a 643 nm wavelength. The difference in ring-down times measured with and without the sample present is used to calculate the experimental extinction coefficient (b_{ext}), as shown by

$$b_{ext} = \frac{R_L}{c} \left(\frac{1}{\tau} - \frac{1}{\tau_0} \right) \tag{4}$$

where R_L is the ratio of the cavity length to the sample length, c is the speed of light, τ_0 is the ring-down time without any particles in the cavity, and τ is the ring-down time when particles are present. Once the extinction coefficient is measured, the particle concentration, N, is measured using a Condensation Particle Counter (CPC). The extinction cross section (σ_{ext}) is calculated according to

$$\sigma_{ext} = \frac{b_{ext,avg}}{N_{avg}} \tag{5}$$

where the subscript avg indicates the average measurement.

To obtain optical growth measurements, we use two cavities connected in series with a homebuilt humidifier between them. Once the particles exit the first cavity, they pass through the humidifier, where the RH of the particles is increased and measured at ~85% in the second cavity. The optical growth factor (fRH) is determined by dividing the extinction cross section of the humidified particles ($\sigma_{ext,a}$) by the extinction cross section of the dry particles ($\sigma_{ext,b}$)

$$fRH(85\% RH, Dry) = \frac{\sigma_{ext,a}}{\sigma_{ext,b}}$$
 (6)

where a is the relative humidity of the humidified particles and b is the relative humidity of the dry particles (<10% RH).

There are currently two methods that are available to calculate a single hygroscopicity parameter from fRH. For the first method, the optical growth factor is converted to the geometric growth factor, G_f , using the experimentally derived refractive indices and Mie theory. G_f has been defined in Equation 2. The diameter of the dry aerosol particles is experimentally selected by the DMA, but the diameter of the humidified particles must be calculated. The humidified diameters are determined by extrapolating the water content of the humidified particle from Mie theory and

the optical growth factor calculation. The first step is to calculate the volume weighted refractive index (m_t) using

$$281 m_t = \sum_i \frac{v_i}{v_t} m_i (7)$$

where V_i is the volume of component i, V_t is the total volume, and m_i is the real portion of the refractive index of the component. Lavallard et al. provided the real part of the refractive index of water at 643 nm I (Lavallard et al. 1996). The imaginary portion of the refractive index is not used since the absorption is negligible at 643 nm. To obtain an extinction coefficient for comparison to the experimentally determined extinction coefficient, extinction coefficients for every particle size 0.1 nm above the dry particle diameter were calculated. The diameter with the lowest variation between the calculated optical growth factor and the experimentally determined optical growth factor is used to calculate the geometric growth factor. Once the growth factor is determined, the κ factor can be calculated using Equation 3. It should be distinguished that the assumptions made for this equation are typically used for supersaturated κ factors where the aerosol particles have very high water content (Taylor et al. 2011; Petters and Kreidenweis 2007).

The second method relates growth factor to optical growth factor through an empirical relationship, as shown by

295
$$fRH(80\%RH, dry) = G_f(80\%RH, dry)^{\frac{0.86}{0.28}}$$
 (8)

where fRH(80%RH, dry) is the optical growth factor at 80% relative humidity, and $G_f(80\%RH, dry)$ is the growth factor at 80% relative humidity. Using Equation 2 and Equation 8, we derive a semi-empirical relation for calculating κ factor as shown by

299
$$\kappa_{Empirical} = \left(\left(fRH(Wet, Dry)^{\frac{3*0.28}{0.86}} \right) - 1 \right) \left(\frac{1 - RH/100}{RH/100} \right)$$
(9)

In the original work by Kreidenweis and Asa-Awuku, this correlation was determined on systems at 80% RH; however, our systems are at ~85% RH. This correlation should be a reasonable approximation at RH < 90%, and has been previously shown to aptly measure the hygroscopicity of organic saccharides measured at 85 % (Dawson et al. 2020; Kreidenweis and Asa-Awuku 2014a).

Modeled Hygroscopicity and Droplet Growth of Mixed Particles

The Zdanovskii-Stokes-Robinson (ZSR) model has been shown to adequately predict the κ -value of binary mixtures (Xu et al. 2020; Jing et al. 2016; Liu et al. 2016; Petters and Kreidenweis 2008; Svenningsson et al. 2006). The basic ZSR model assumes volume additivity, and determines the κ of a mixed system based on the volume fraction of each species (ϵ_i) as shown in Equation 10.

311
$$\kappa_{ZSR} = \sum_{i} \epsilon_i \kappa_i$$
 (10)

Equation 4 works well for infinitely soluble species, but fails to predict the water-uptake of a system when sparingly soluble organics are present (Petters and Kreidenweis 2008; Bilde and Svenningsson 2004). Hence, for such mixtures, the limited solubility of particles must be considered as it can affect the apparent κ . Changes in κ due to limited solubility can be captured by including a dissolved volume fraction term ($H(x_i)$), by doing so, turning Equation 10 into

317 Equation 11:

318
$$\kappa_{ZSR,Ci} = \sum_{i} \epsilon_i \kappa_i H(x_i)$$

319
$$H(x_i) = \begin{cases} x_i \ x_i < 1 \\ 1 \ x_i \ge 1 \end{cases} \tag{11}$$

$$320 x_i = C_i \left(\frac{V_w}{V_{si}} \right)$$

- Where C_i , V_w , and V_{si} are the solubility of solute in water (volume of compound per unit volume of water), volume of water, and volume of the dry aerosol (soluble and insoluble) (Petters and Kreidenweis 2008). Alternatively, C_i in Equation 11 can also be estimated based on their O:C through the empirical relationship in Equation 12 which assumes that the water-uptake activity of sufficiently soluble compounds can be estimated by Raoult's law, and that O:C and molecular size
- determine the volatility of the organic compound (Nakao 2017).

$$327 \quad lnC_{empirical} = 20 \left[\left(\frac{o}{c} \right)^{0.402} - 1 \right] \quad ; \quad x_i = C_{empirical} \left(\frac{V_w}{V_{si}} \right)$$
 (12)

- Where O and C are the number of oxygen and carbon atoms in the molecule. Based on Equation
- 329 (12), the solubility range corresponds to O:C range of 0.2 to 0.7. The theoretical κ -value based on
- this empirically derived solubility will hereinafter be referred to as $\kappa_{ZSR,emp}$. For infinitely soluble
- species, $H(x_i) = 1$, and so $\kappa_{ZSR} = \kappa_{ZSR,Ci} = \kappa_{ZSR,emp}$.
- In this work, calculated κ of pure levoglucosan, sucrose, adipic acid, and ammonium sulfate was
- 333 used in all three versions of the ZSR models to predict the hygroscopicity and particle growth of
- 334 the mixtures. Levoglucosan and adipic acid were predicted to be affected by limited solubility,
- 335 whereas sucrose would behave as an infinitely soluble particle. Lastly, to compare measured κ -
- values to the three variations of the ZSR model, a normalized mean error (NME) analysis was
- done using the equation below:

338
$$NME = \frac{\sum_{1}^{n} |\kappa_{model} - \kappa_{measured}|}{\sum_{1}^{n} (\kappa_{measured})}$$
 (13)

339 A NME <10% suggests that the model agrees with the data in most instances. The model that leads 340 to the least NME between measured and predicted κ -values was then taken to be the best model 341 for the system.

RESULTS AND DISCUSSION

342

343

Water-Uptake of Internal Mixtures

As previously mentioned, intercomparisons of the hygroscopicities of ammonium sulfateorganic binary mixtures were done by retrieving κ from the measured parameters (D_{p50} , G_f , fRH). Here, experimental κ -values were compared across instruments and with the ZSR-predicted κ with and without limited solubility considerations (Figure 3).

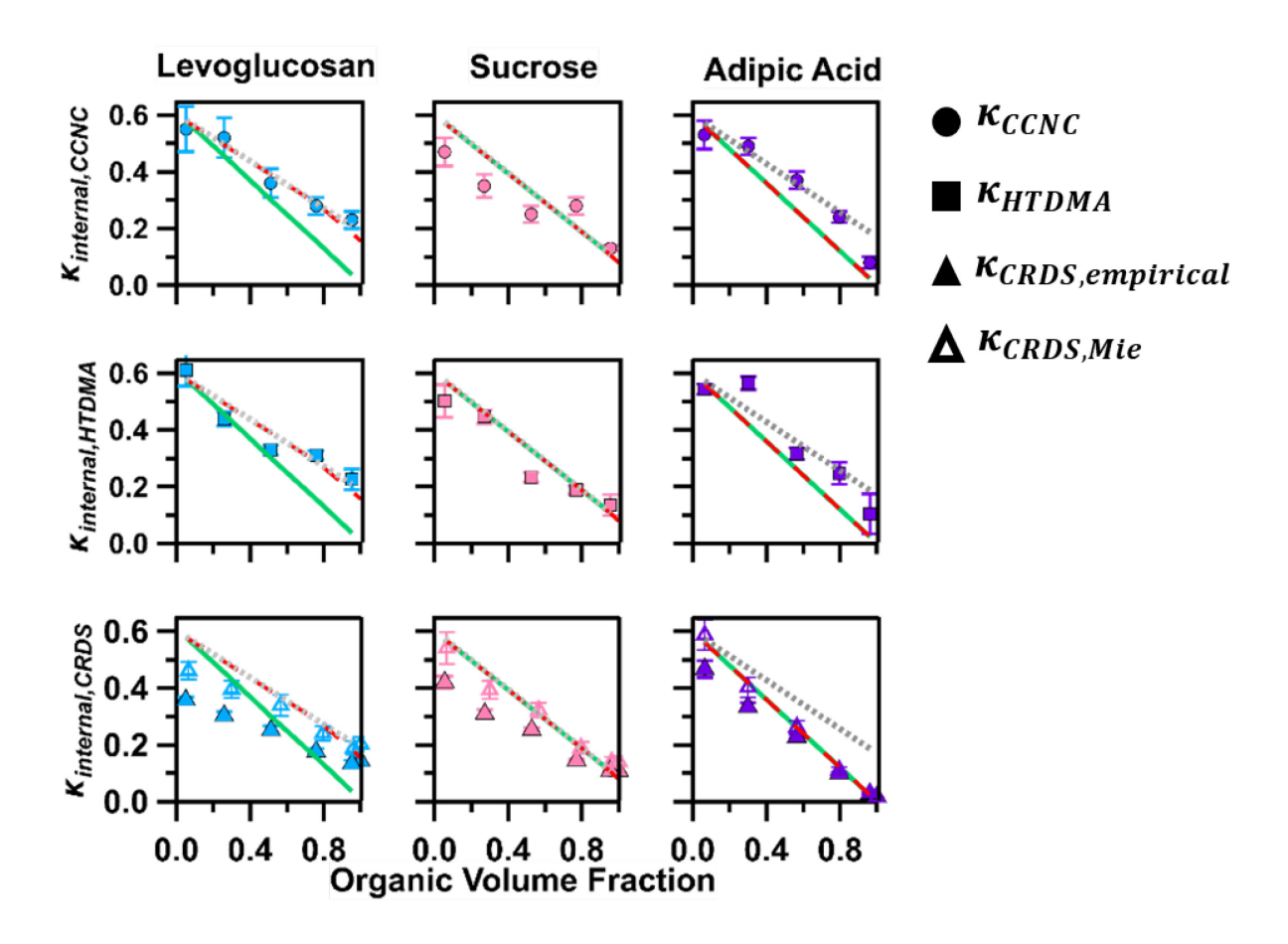


Figure 3 Comparison of experimental to ZSR-predicted κ values based on assumptions of infinite solubility as described in Equation 10 (grey dotted), limited solubility as described in Equation 11 (green), and the O:C limited solubility (red dashed) as described in Equation 12 for levoglucosan (blue), sucrose (pink), and adipic acid (purple) binary mixtures as measured by the CCNC (circle), HTDMA (square), and CRDS with Mie theory based (open triangle) and empirical (solid triangle) κ -retrieval methods.

Normalized mean error analysis results are presented in Table 2. For levoglucosan-ammonium

sulfate internal mixtures, $\kappa_{ZSR,Ci}$ poorly predicted hygroscopicity, with a NME that was higher than the two other models. κ_{ZSR} and $\kappa_{ZSR,emp}$ were identical for levoglucosan-ammonium sulfate aerosol particles with organic volume fractions < 0.8. At higher organic volume fractions, $\kappa_{ZSR,emp}$ predicted that limited solubility would affect the particle water-uptake at supersaturated

conditions. However, the effect is small, as κ_{ZSR} and $\kappa_{ZSR,emp}$ agreed within 10% uncertainty. Experimentally, internally mixed levoglucosan-ammonium sulfate particles took up water as expected for infinitely soluble species. NME analysis shows that in the scope of our experimental conditions, internally mixed levoglucosan-ammonium sulfate aerosol particles were not limited by solubility at the supersaturated regime and at the RH of the HTDMA as measured κ_{CCNC} and κ_{HTDMA} were able to be predicted by κ_{ZSR} with < 10% uncertainty. The inability of $\kappa_{ZSR,Ci}$ to capture measured hygroscopicity of ammonium sulfate-levoglucosan suggests that the use of bulk solubility may be inaccurate for ammonium sulfate-levoglucosan droplet growth predictions. This inaccuracy when using bulk solubility to capture particle hygroscopicity is consistent with recent literature that have shown changes in supramolecular interactions under supersaturated conditions that lead to changes in hygroscopicity (Wallace et al. 2021; Richards et al. 2020). As the HTDMA and CRDS were operated at similar RH, their κ -values were expected to be invariant, however, $\kappa_{CRDS,Mie}$ was significantly lower. κ_{ZSR} and $\kappa_{ZSR,emp}$ overpredicted $\kappa_{CRDS,Mie}$ by an average of 20%, with the largest error at organic fractions < 0.5, which may simply be due to fluctuations in RH. In summary, internally mixed levoglucosan-ammonium sulfate particles were found to behave as fully soluble particles, and water-uptake measurements using the CCNC and HTDMA were able to be well-predicted by κ_{ZSR} and $\kappa_{ZSR.emp}$. Additionally, $\kappa_{ZSR.Ci}$ that is calculated based on the organic's bulk solubility was not a good predictor of levoglucosan-ammonium sulfate wateruptake and had an uncertainty of over 20%. Sucrose is a highly soluble (2040 g L⁻¹) organic compound with relatively low

360

361

362

363

364

365

366

367

368

369

370

371

372

373

374

375

376

377

378

379

380

381

382

hygroscopicity compared to ammonium sulfate (Table 1). Due to the high solubility of sucrose, for calculations of $\kappa_{ZSR,Ci}$, $H(x_i)=1$ which leads to $\kappa_{ZSR}=\kappa_{ZSR,Ci}$ as can be seen in Figure 3. However, $\kappa_{ZSR,emp}$ of sucrose slightly varied from κ_{ZSR} at organic volume fractions > 0.75,

suggesting that sucrose may not be fully soluble at under such conditions. However, the difference between $\kappa_{ZSR,emp}$ and κ_{ZSR} is insignificant, with <1 % difference between the NME of κ_{ZSR} and $\kappa_{ZSR,emp}$ of sucrose (Table 2). In the scope of this paper, predictions of internally mixed sucrose-ammonium sulfate water-uptake by all three versions of the ZSR models are considered statistically invariant (Figure 3). In other words, sucrose droplet predictions and water uptake are not affected by limited solubility. Measured subsaturated water-uptake of internally mixed sucrose-ammonium sulfate particles agreed (within 15% uncertainty) with ZSR predictions. In contrast, uncertainty doubled for supersaturated measurements (Table 2), and κ_{CCNC} values were overpredicted at organic volume fractions < 0.75. This overprediction suggests that at supersaturated conditions, ammonium sulfate and sucrose components do not have equal contributions as suggested by ZSR. It is likely that other factors such as morphology may affect the water-uptake properties of mixed particles as it can promote adsorption driven droplet growth instead of solute driven (ZSR) droplet growth (Barati et al. 2019; Hatch et al. 2008).

In the case of internally mixed adipic acid and ammonium sulfate, $\kappa_{ZSR,Ci}$ and $\kappa_{ZSR,emp}$ were statistically invariant and are shown as overlapping green and red lines in Figure 3. κ_{CCNC} and κ_{HTDMA} of internally mixed adipic acid-ammonium sulfate agreed with κ_{ZSR} , suggesting that solubility did not affect particle water-uptake. In contrast, $\kappa_{CRDS,Mie}$ was able to be accurately predicted by $\kappa_{ZSR,Ci}$ and $\kappa_{ZSR,emp}$.

Table 2 Normal mean error analysis of binary internally mixed particle water-uptake

Normal Mean Error, kZSR (%)				
Method Organic	CCNC	нтрма	CRDS, mie	CRDS, empirical
Levoglucosan	6.0%	9.8%	19.8%	60.9%
Sucrose	26.4%	14.7%	9.5%	35.4%
Adipic Acid	11.7%	14.5%	34.3%	59.3%
Normal Mean Error, kZSR - limited solubility (%)				
Levoglucosan	24.2%	22.0%	28.4%	44.3%
Sucrose	26.4%	14.7%	9.5%	35.4%
Adipic Acid	22.6%	23.9%	4.5%	20.8%
Normal Mean Error, kZSR - O:C limited solubility (%)				
Levoglucosan	7.2%	11.1%	20.2%	58.4%
Sucrose	26.5%	14.8%	9.6%	35.5%
Adipic Acid	22.6%	23.8%	4.5%	20.8%

Note that 2 values of κ_{CRDS} were retrieved from fRH measurements ($\kappa_{CRDS,mie}$ and $\kappa_{CRDS,emp}$) as previously detailed. Values of $\kappa_{CRDS,mie}$ and $\kappa_{CRDS,emp}$ for binary internal mixtures have been found to be comparable for single-component systems (Dawson et al. 2020). However, for internally mixed inorganic-organic aerosols, $\kappa_{CRDS,emp}$ was consistently less than its Mie theory derived counterpart. $\kappa_{CRDS,emp}$ of ammonium sulfate-adipic acid was able to be adequately captured by the ZSR models within ~20%. This deviation is likely because the empirical method of κ retrieval from fRH was formulated based on fRH measurements done at 80% RH with limited experimental data, whereas in this work, RH was set at 85% (Dawson et al. 2020; Kreidenweis and Asa-Awuku 2014a). Although κ -values are RH independent, the empirical relationship is sensitive to limited solubility and thus dependent on RH. The relationship was developed with ammonium sulfate and has been shown to hold for sucrose but may deviate for other compounds with limited solubility measured at different RH. The range of solubilities and RH that the empirical relationship can be used for is a direction for future studies.

Water-Uptake of External Mixtures

As stated above, the water-uptake of two distinct externally mixed populations may be exhibited in the measurement outputs (Fig 2). For CCNC and HTDMA, ideally, each chemical component of an external mixture can be distinguished as each species would have its own κ -value. In the case of binary mixtures, externally mixed particles would result in two κ -values, one of ammonium sulfate ($\kappa_{ammonium \, sulfate} = \sim 0.6$) and one of the organic. However, for CRDS, the average of measured signal results in a single average fRH and κ -value. Figure 5 shows the experimental results for externally mixed particle hygroscopicity.

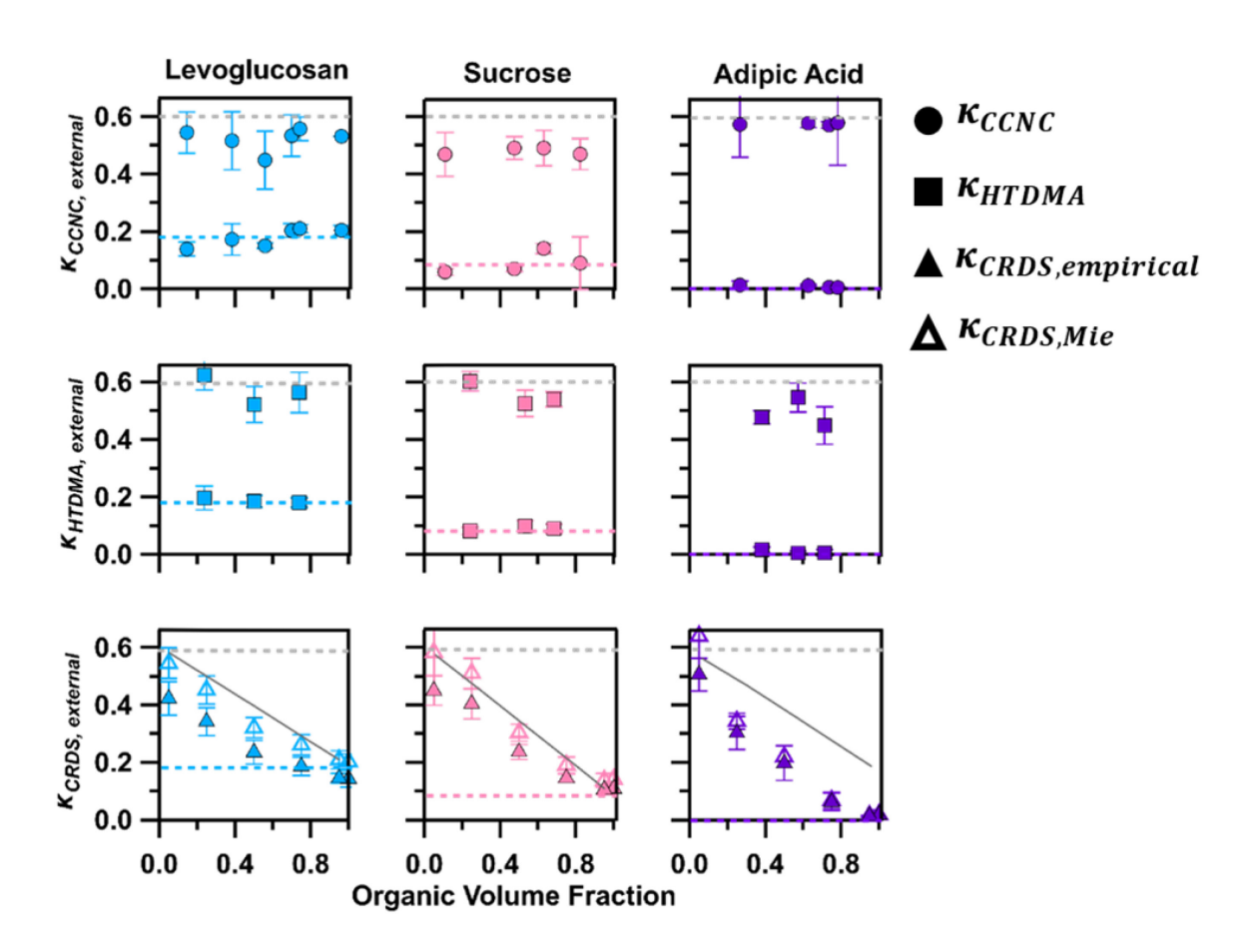


Figure 4 κ values of binary external mixtures of ammonium sulfate and levoglucosan (blue), sucrose (pink) and adipic acid (purple) as measured by the CCNC (circle), HTDMA (square), and CRDS (triangle). κ_{CRDS} was retrieved based on an empirical method (solid symbols) and Mie theory (open symbols). κ of pure ammonium sulfate (grey) and organics are shown as dashed lines. κ_{ZSR} (solid grey line) is shown with $\kappa_{CRDS,external}$

All measured κ_{CCNC} and κ_{HTDMA} values of externally mixed ammonium sulfate and organics were able to show the presence of two externally mixed compounds (Figure 4). In the case of binary mixtures, each mixture composition resulted in two distinct κ_{CCNC} and κ_{HTDMA} values. The first κ -value was consistent with $\kappa_{ammonium\,sulfate}$ (0.6) and the second was consistent with the organic compound. A striking observation was made in $\kappa_{\textit{CCNC}}$ of externally mixed ammonium sulfate-sucrose. Although one of the measured κ -value was consistent with that of sucrose, its inorganic counterpart was consistently lower than $\kappa_{ammonium \, sulfate}$. Recall that similar overpredictions were observed in the κ_{CCNC} of internally mixed ammonium sulfate-sucrose as well. This further suggests that sucrose may affect droplet formation of mixed particles beyond solubility. As sucrose can be viscous, this property may affect the droplet formation of the mixture and should be probed in future studies. In contrast, CRDS-derived κ -values for all mixtures were based on the average signal measured during the cavity ring-down measurements. As such, there were no distinguishable differences in the average κ_{CRDS} -values of the external and internal mixtures. Any variation between internal and external κ -values from the CRDS is most likely from background noise in the measurements and are reflected in the error bars.

429

430

431

432

433

434

435

436

437

438

439

440

441

442

443

444

445

446

447

448

There was no clear indication of external mixing and κ -values of internal and externally mixed particles were statistically invariable. This aspect of the cavity ring-down method is an important consideration when utilizing the instrument to measure the water-uptake of an unknown system such as ambient air. The average hygroscopicity value will provide the average water-uptake of the aerosol system but will not indicate the mixing state of the system.

SUMMARY

449

450

451

452

453

454

455

456

457

458

459

460

461

462

463

464

465

466

467

The water-uptake of mixed inorganic-organic systems is complex and is influenced by the solubility, viscosity, hydrophobicity, and surface activity (Xu et al. 2021; Tandon et al. 2018; Petters and Kreidenweis 2008). In this work, hygroscopicity of binary inorganic-organic mixtures was compared across three instrumental methods, four κ retrieval methods, and under sub- and supersaturated conditions. For internally mixed ammonium sulfate-organic mixtures, CCNC and HTDMA measured hygroscopicities were in good agreement, and for externally mixed aerosols, the two methods were able to show the presence of two distinct, pure particle populations, a key characteristic of external mixtures. Additionally, this work is the first to compare three versions of the ZSR model and shows that for some internally mixed particles such as the ammonium sulfatelevoglucosan mixtures, the use of bulk solubility $(\kappa_{ZSR,Ci})$ is not always accurate. This work shows that different instruments can have complementary advantages, and to get a clearer picture of mixed aerosol particle hygroscopicity, the use of more than one instrument is highly advisable. For example, when measuring complex systems such as ambient aerosols, the use of cavity ringdown can measure the average water-uptake of a system, but to gain insight on particle mixing states, it must be coupled with a CCNC or HTDMA. The results in this work may provide more insight into the perceived hygroscopicity of complex mixtures and supports the development of future high-resolution hygroscopicity measurement methods.

DATA AVAILABILITY

The data is available upon request from the corresponding authors as stated.

469	AUTHOR CONTRIBUTIONS
470	PNR and KAM, TMR, DD, AAA designed and conducted the CCN and H-TDMA experiments.
471	KD, JND and MAF conducted experiments, and performed the calculations using the CRDS
472	data. PNR conducted modelling analysis across all three data sets and prepared the manuscript
473	with input from all the co-authors.
474	COMPETING INTERESTS
475	The authors declare that they have no conflict of interest.
476	ACKNOWLEDGEMENTS
., .	
477	PNR, KAM, and AAA acknowledge support from the NSF: AGS-1723920 and AGS-2124489.
478	KD, JND, MAF acknowledge support from NSF: AGS-2124490. PNR and JND also
479	acknowledge support from NSF GRFP Awards (1840340 & 1255832). DD and TMR
480	acknowledge support from the NSF: AGS-2124491.
481	ORCID
482	Patricia N. Razafindrambinina: 0000-0002-1553-5839
483	Kotiba A. Malek: 0000-0002-9326-3859
484	Dabrina D Dutcher: 0000-0001-9084-6621
485	Timothy M. Raymond: 0000-0002-3821-2020
486	Miriam A. Freedman: 0000-0003-4374-6518
487	Akua A. Asa-Awuku: 0000-0002-0354-8368
488	

489	REFERENCES
490	Abbatt, J.P.D., Broekhuizen, K., and Pradeep Kumar, P. (2005). Cloud condensation nucleus
491	activity of internally mixed ammonium sulfate/organic acid aerosol particles. Atmospheric
492	Environment 39 (26):4767-4778. doi:10.1016/j.atmosenv.2005.04.029.
493	Altaf, M.B., Dutcher, D.D., Raymond, T.M., and Freedman, M.A. (2018). Effect of Particle
494	Morphology on Cloud Condensation Nuclei Activity. ACS Earth and Space Chemistry 2
495	(6):634–639. doi:10.1021/acsearthspacechem.7b00146.
496	Barati, F., Yao, Q., and Asa-Awuku, A.A. (2019). Insight into the Role of Water-Soluble
497	Organic Solvents for the Cloud Condensation Nuclei Activation of Cholesterol. ACS Earth
498	and Space Chemistry 3 (9):1697-1705. doi:10.1021/acsearthspacechem.9b00161.
499	Bilde, M. and Svenningsson, B. (2004). CCN activation of slightly soluble organics: the
500	importance of small amounts of inorganic salt and particle phase. Tellus B: Chemical and
501	Physical Meteorology 56 (2):128–134. doi:10.3402/tellusb.v56i2.16406.
502	Broekhuizen, K., Kumar, P.P., and Abbatt, J.P.D. (2004). Partially soluble organics as cloud
503	condensation nuclei: Role of trace soluble and surface active species. Geophysical Research
504	Letters 31 (1):1-5. doi:10.1029/2003GL018203.
505	Brooks, S.D., Wise, M.E., Cushing, M., and Tolbert, M.A. (2002). Deliquescence behavior of
506	organic/ammonium sulfate aerosol. Geophysical Research Letters 29 (19):2-5.
507	doi:10.1029/2002GL014733.
508	Cruz, C.N. and Pandis, S.N. (2000). Deliquescence and Hygroscopic Growth of Mixed
509	Inorganic-Organic Atmospheric Aerosol.

510	Cruz, C.N. and Pandis, S.N. (1998). The effect of organic coatings on the cloud condensation
511	nuclei activation of inorganic atmospheric aerosol. Journal of Geophysical Research
512	Atmospheres 103 (D11):13111-13123. doi:10.1029/98JD00979.
513	Dawson, J.N., Malek, K.A., Razafindrambinina, P.N., Raymond, T.M., Dutcher, D.D., Asa-
514	Awuku, A.A., and Freedman, M.A. (2020). Direct Comparison of the Submicron Aerosol
515	Hygroscopicity of Water-Soluble Sugars. ACS Earth and Space Chemistry.
516	doi:10.1021/acsearthspacechem.0c00159.
517	Freedman, M.A., Hasenkopf, C.A., Beaver, M.R., and Tolbert, M.A. (2009). Optical properties
518	of internally mixed aerosol particles composed of dicarboxylic acids and ammonium
519	sulfate. Journal of Physical Chemistry A 113 (48):13584–13592. doi:10.1021/jp906240y.
520	Hatch, C.D., Gierlus, K.M., Schuttlefield, J.D., and Grassian, V.H. (2008). Water adsorption and
521	cloud condensation nuclei activity of calcite and calcite coated with model humic and fulvic
522	acids. Atmospheric Environment 42 (22):5672–5684. doi:10.1016/j.atmosenv.2008.03.005.
523	Hays, M.D., Geron, C.D., Linna, K.J., Smith, N.D., and Schauer, J.J. (2002). Speciation of gas-
524	phase and fine particle emissions from burning of foliar fuels. Environ Sci Technol 36
525	(11):2281–2295. doi:10.1021/es0111683.
526	Haywood, J. and Boucher, O. (2000). Estimates of the direct and indirect radiative forcing due to
527	tropospheric aerosols: A review. Reviews of Geophysics 38 (4):513-543.
528	doi:10.1029/1999RG000078.
529	IPCC (2021). Climate Change 2021: The Physical Science Basis. Contribution of Working
530	Group I to the Sixth Assessment Report of the Intergovernmental Panel on Climate Change,
531	Cambridge University Press.

532 Jimenez, J.L., Canagaratna, M.R., Donahue, N.M., Prevot, A.S.H., Zhang, Q., Kroll, J.H., 533 DeCarlo, P.F., Allan, J.D., Coe, H., Ng, N.L., Aiken, A.C., Docherty, K.S., Ulbrich, I.M., 534 Grieshop, A.P., Robinson, A.L., Duplissy, J., Smith, J.D., Wilson, K.R., Lanz, V.A., 535 Hueglin, C., Sun, Y.L., Tian, J., Laaksonen, A., Raatikainen, T., Rautiainen, J., Vaattovaara, 536 P., Ehn, M., Kulmala, M., Tomlinson, J.M., Collins, D.R., Cubison, M.J., Dunlea, J., 537 Huffman, J.A., Onasch, T.B., Alfarra, M.R., Williams, P.I., Bower, K., Kondo, Y., 538 Schneider, J., Drewnick, F., Borrmann, S., Weimer, S., Demerjian, K., Salcedo, D., Cottrell, 539 L., Griffin, R., Takami, A., Miyoshi, T., Hatakeyama, S., Shimono, A., Sun, J.Y., Zhang, 540 Y.M., Dzepina, K., Kimmel, J.R., Sueper, D., Jayne, J.T., Herndon, S.C., Trimborn, A.M., 541 Williams, L.R., Wood, E.C., Middlebrook, A.M., Kolb, C.E., Baltensperger, U., and 542 Worsnop, D.R. (2009). Evolution of Organic Aerosols in the Atmosphere. Science (1979) 543 326 (5959):1525 LP – 1529. doi:10.1126/science.1180353. 544 Jing, B., Tong, S., Liu, Q., Li, K., Wang, W., Zhang, Y., and Ge, M. (2016). Hygroscopic 545 behavior of multicomponent organic aerosols and their internal mixtures with ammonium 546 sulfate. Atmospheric Chemistry and Physics 16 (6):4101–4118. doi:10.5194/acp-16-4101-547 2016. 548 Kanakidou, M., Seinfeld, J.H., Pandis, S.N., Barnes, I., Dentener, F.J., Facchini, M.C., Van 549 Dingenen, R., Ervens, B., Nenes, A., Nielsen, C.J., Swietlicki, E., Putaud, J.P., Balkanski, 550 Y., Fuzzi, S., Horth, J., Moortgat, G.K., Winterhalter, R., Myhre, C.E.L., Tsigaridis, K., 551 Vignati, E., Stephanou, E.G., and Wilson, J. (2005). Organic aerosol and global climate 552 modelling: A review. Atmospheric Chemistry and Physics 5 (4):1053–1123. 553 doi:10.5194/acp-5-1053-2005.

554 Kaplan, I.R. and Kawamura, K. (1987). Motor Exhaust Emissions as a Primary Source for 555 Dicarboxylic Acids in Los Angeles Ambient Air. Environmental Science and Technology 556 21 (1):105–110. doi:10.1021/es00155a014. 557 Kreidenweis, S.M. and Asa-Awuku, A. (2014a). Aerosol hygroscopicity: Particle water content 558 and its role in atmospheric processes. 559 Kreidenweis, S.M. and Asa-Awuku, A. (2014b). Aerosol hygroscopicity: Particle water content 560 and its role in atmospheric processes. 561 Lavallard, P., Rosenbauer, M., and Gacoin, T. (1996). Influence of surrounding dielectrics on the 562 spontaneous emission of sulforhodamine B molecules. *Physical Review A - Atomic*, 563 Molecular, and Optical Physics 54 (6):5450–5453. doi:10.1103/PhysRevA.54.5450. 564 Lei, T., Zuend, A., Wang, W.G., Zhang, Y.H., and Ge, M.F. (2014a). Hygroscopicity of organic 565 compounds from biomass burning and their influence on the water uptake of mixed organic 566 ammonium sulfate aerosols. Atmospheric Chemistry and Physics 14 (20):11165–11183. 567 doi:10.5194/acp-14-11165-2014. 568 Lei, T., Zuend, A., Wang, W.G., Zhang, Y.H., and Ge, M.F. (2014b). Hygroscopicity of organic 569 compounds from biomass burning and their influence on the water uptake of mixed organic 570 ammonium sulfate aerosols. Atmospheric Chemistry and Physics 14 (20):11165–11183. 571 doi:10.5194/acp-14-11165-2014. 572 Liu, Q., Jing, B., Peng, C., Tong, S., Wang, W., and Ge, M. (2016). Hygroscopicity of internally 573 mixed multi-component aerosol particles of atmospheric relevance. Atmospheric 574 Environment 125:69–77. doi:10.1016/j.atmosenv.2015.11.003.

575	Lohmann, U. and Feichter, J. (2005). Atmospheric Chemistry and Physics Global indirect
576	aerosol effects: a review. Atmos. Chem. Phys 5:715-737.
577	Marcolli, C., Luo, B., Peter, T., and Wienhold, F.G. (2004). Internal mixing of the organic
578	aerosol by gas phase diffusion of semivolatile organic compounds. Atmospheric Chemistry
579	and Physics Discussions 4 (5):5789-5806. doi:10.5194/acpd-4-5789-2004.
580	Marynowski, L. and Simoneit, B.R.T. (2022). Saccharides in atmospheric particulate and
581	sedimentary organic matter: Status overview and future perspectives. Chemosphere 288
582	(P1):132376. doi:10.1016/j.chemosphere.2021.132376.
583	Mikhailov, E.F. and Vlasenko, S.S. (2020). High-humidity tandem differential mobility analyzer
584	for accurate determination of aerosol hygroscopic growth, microstructure, and activity
585	coefficients over a wide range of relative humidity. Atmospheric Measurement Techniques
586	13 (4):2035–2056. doi:10.5194/amt-13-2035-2020.
587	Moore, R.H. and Nenes, A. (2009). Scanning flow CCN analysis method for fast measurements
588	of CCN spectra. Aerosol Science and Technology 43 (12):1192-1207.
589	doi:10.1080/02786820903289780.
590	Nakao, S. (2017). Why would apparent κ linearly change with O/C? Assessing the role of
591	volatility, solubility, and surface activity of organic aerosols. Aerosol Science and
592	Technology 51 (12):1377–1388. doi:10.1080/02786826.2017.1352082.
593	Nandy, L., Yao, Y., Zheng, Z., and Riemer, N. (2021). Water uptake and optical properties of
594	mixed organic-inorganic particles. Aerosol Science and Technology 55 (12):1398–1413.
595	doi:10.1080/02786826.2021.1966378.

596	Ott, E.J.E., Tackman, E.C., and Freedman, M.A. (2020). Effects of Sucrose on Phase Transitions
597	of Organic/Inorganic Aerosols. ACS Earth and Space Chemistry 4 (4):591-601.
598	doi:10.1021/acsearthspacechem.0c00006.
599	Padró, L.T., Moore, R.H., Zhang, X., Rastogi, N., Weber, R.J., and Nenes, A. (2012). Mixing
500	state and compositional effects on CCN activity and droplet growth kinetics of size-resolved
501	CCN in an urban environment. Atmospheric Chemistry and Physics 12 (21):10239–10255.
502	doi:10.5194/acp-12-10239-2012.
503	Pashynska, V., Vermeylen, R., Vas, G., Maenhaut, W., and Claeys, M. (2002). Development of a
504	gas chromatographic/ion trap mass spectrometric metod for the determination of
505	levoglucosan and saccharidic compounds in atmospheric aerosols. Application to urban
506	aerosols. Journal of Mass Spectrometry 37 (12):1249–1257. doi:10.1002/jms.391.
507	Petters, M.D. and Kreidenweis, S.M. (2013). A single parameter representation of hygroscopic
508	growth and cloud condensation nucleus activity-Part 3: Including surfactant partitioning.
509	Atmospheric Chemistry and Physics 13 (2):1081–1091. doi:10.5194/acp-13-1081-2013.
510	Petters, M.D. and Kreidenweis, S.M. (2008). A single parameter representation of hygroscopic
511	growth and cloud condensation nucleus activity - Part 2: Including solubility. Atmospheric
512	Chemistry and Physics 8 (20):6273-6279. doi:10.5194/acp-8-6273-2008.
513	Petters, M.D. and Kreidenweis, S.M. (2007). A single parameter representation of hygroscopic
514	growth and cloud condensation nucleus activity. Atmospheric Chemistry and Physics 7
515	(8):1961–1971. doi:10.5194/acp-7-1961-2007.

616 Prenni, A.J., DeMott, P.J., Kreidenweis, S.M., Sherman, D.E., Russell, L.M., and Ming, Y. 617 (2001). The effects of low molecular weight dicarboxylic acids on cloud formation. Journal 618 of Physical Chemistry A 105 (50):11240–11248. doi:10.1021/jp012427d. 619 Prenni, A.J., Petters, M.D., Kreidenweis, S.M., DeMott, P.J., and Ziemann, P.J. (2007). Cloud 620 droplet activation of secondary organic aerosol. Journal of Geophysical Research 621 Atmospheres 112 (10). doi:10.1029/2006JD007963. 622 Raymond, T.M. and Pandis, S.N. (2003). Formation of cloud droplets by multicomponent 623 organic particles. Journal of Geophysical Research D: Atmospheres 108 (15). 624 doi:10.1029/2003jd003503. 625 Razafindrambinina, P.N., Malek, K.A., Dawson, J.N., DiMonte, K., Raymond, T.M., Dutcher, 626 D.D., Freedman, M.A., and Asa-Awuku, A. (2022). Hygroscopicity of Internally Mixed 627 Ammonium Sulfate and Secondary Organic Aerosol Particles Formed at Low and High 628 Relative Humidity. Environmental Science: Atmospheres. doi:10.1039/d1ea00069a. 629 Richards, D.S., Trobaugh, K.L., Hajek-Herrera, J., Price, C.L., Sheldon, C.S., Davies, J.F., and 630 Davis, R.D. (2020). Ion-molecule interactions enable unexpected phase transitions in 631 organic-inorganic aerosol, Sci. Adv. 632 Rickards, A.M.J., Miles, R.E.H., Davies, J.F., Marshall, F.H., and Reid, J.P. (2013). 633 Measurements of the sensitivity of aerosol hygroscopicity and the κ parameter to the O/C 634 ratio. Journal of Physical Chemistry A 117 (51):14120–14131. doi:10.1021/jp407991n. 635 Riemer, N., Ault, A.P., West, M., Craig, R.L., and Curtis, J.H. (2019). Aerosol Mixing State: 636 Measurements, Modeling, and Impacts. Reviews of Geophysics 57 (2):187–249. 637 doi:10.1029/2018RG000615.

638 Rose, D., Gunthe, S.S., Mikhailov, E., Frank, G.P., Dusek, U., Andreae, M.O., and Pöschl, U. 639 (2008). Calibration and measurement uncertainties of a continuous-flow cloud condensation 640 nuclei counter (DMT-CCNC): CCN activation of ammonium sulfate and sodium chloride 641 aerosol particles in theory and experiment. Atmospheric Chemistry and Physics 8 (5):1153– 642 1179. doi:10.5194/acp-8-1153-2008. 643 Rosenørn, T., Kiss, G., and Bilde, M. (2006). Cloud droplet activation of saccharides and 644 levoglucosan particles. Atmospheric Environment 40 (10):1794–1802. 645 doi:10.1016/j.atmosenv.2005.11.024. 646 Schill, S.R., Collins, D.B., Lee, C., Morris, H.S., Novak, G.A., Prather, K.A., Quinn, P.K., 647 Sultana, C.M., Tivanski, A. V., Zimmermann, K., Cappa, C.D., and Bertram, T.H. (2015). 648 The impact of aerosol particle mixing state on the hygroscopicity of sea spray aerosol. ACS 649 Central Science 1 (3):132–141. doi:10.1021/acscentsci.5b00174. 650 Svenningsson, B., Rissler, J., Swietlicki, E., Mircea, M., Bilde, M., Facchini, M.C., Decesari, S., 651 Fuzzi, S., Zhou, J., Mønster, J., and Rosenørn, T. (2006). Hygroscopic growth and critical 652 supersaturations for mixed aerosol particles of inorganic and organic compounds of 653 atmospheric relevance. Atmospheric Chemistry and Physics 6 (7):1937–1952. 654 doi:10.5194/acp-6-1937-2006. 655 Tandon, A., Rothfuss, N. El, and Petters, M. (2018). The effect of hydrophobic glassy organic 656 material on the cloud condensation nuclei activity of internally mixed particles with 657 different particle morphologies. Atmospheric Chemistry and Physics Discussions (16):1–24. 658 doi:10.5194/acp-2018-831.

659	Taylor, N.F., Collins, D.R., Spencer, C.W., Lowenthal, D.H., Zielinska, B., Samburova, V., and
660	Kumar, N. (2011). Measurement of ambient aerosol hydration state at Great Smoky
661	Mountains National Park in the southeastern United States. Atmospheric Chemistry and
662	Physics 11 (23):12085-12107. doi:10.5194/acp-11-12085-2011.
663	VanReken, T.M., Ng, N.L., Flagan, R.C., and Seinfeld, J.H. (2005). Cloud condensation nucleus
664	activation properties of biogenic secondary organic aerosol. Journal of Geophysical
665	Research Atmospheres 110 (7):1–9. doi:10.1029/2004JD005465.
666	Veghte, D.P. and Freedman, M.A. (2012). The necessity of microscopy to characterize the
667	optical properties of size-selected, nonspherical aerosol particles. Analytical Chemistry 84
668	(21):9101–9108. doi:10.1021/ac3017373.
669	Vu, D., Gao, S., Berte, T., Kacarab, M., Yao, Q., Vafai, K., and Asa-Awuku, A. (2019). External
670	and internal cloud condensation nuclei (CCN) mixtures: Controlled laboratory studies of
671	varying mixing states. Atmospheric Measurement Techniques 12 (8):4277–4289.
672	doi:10.5194/amt-12-4277-2019.
673	Wallace, B.J., Price, C.L., Davies, J.F., and Preston, T.C. (2021). Multicomponent diffusion in
674	atmospheric aerosol particles. Environmental Science: Atmospheres 1 (1):45-55.
675	doi:10.1039/D0EA00008F.
676	Wex, H., Petters, M.D., Carrico, C.M., Hallbauer, E., Massling, A., McMeeking, G.R., Poulain,
677	L., Wu, Z., Kreidenweis, S.M., and Stratmann, F. (2009). Towards closing the gap between
678	hygroscopic growth and activation for secondary organic aerosol: Part 1-Evidence from
679	measurements. Atmospheric Chemistry and Physics 9 (12):3987-3997. doi:10.5194/acp-9-
680	3987-2009.

681 Xu, W., Fossum, K.N., Ovadnevaite, J., Lin, C., Huang, R., Dowd, C.O., and Ceburnis, D. 682 (2021). The impact of aerosol size-dependent hygroscopicity and mixing state on the cloud 683 condensation nuclei potential over the Northeast Atlantic. Atmospheric Chemistry and 684 Physics Discussions (February):1–31. 685 Xu, W., Ovadnevaite, J., Fossum, K.N., Lin, C., Huang, R.J., O'Dowd, C., and Ceburnis, D. 686 (2020). Aerosol hygroscopicity and its link to chemical composition in the coastal 687 atmosphere of Mace Head: Marine and continental air masses. Atmospheric Chemistry and 688 Physics 20 (6):3777–3791. doi:10.5194/acp-20-3777-2020. 689 Yttri, K.E., Dye, C., and Kiss, G. (2007). Ambient aerosol concentrations of sugars and sugar-690 alcohols at four different sites in Norway. Atmospheric Chemistry and Physics 7 (16):4267– 691 4279. doi:10.5194/acp-7-4267-2007. 692 Zardini, A.A., Sjogren, S., Marcolli, C., Krieger, U.K., Gysel, M., Weingartner, E., 693 Baltensperger, U., and Peter, T. (2008). A combined particle trap/HTDMA hygroscopicity 694 study of mixed inorganic/organic aerosol particles. Atmospheric Chemistry and Physics 8 695 (18):5589-5601. doi:10.5194/acp-8-5589-2008. 696 Zhang, F., Li, Z., Li, Y., Sun, Y., Wang, Z., Li, P., Sun, L., Wang, P., Cribb, M., Zhao, C., Fan, 697 T., Yang, X., and Wang, Q. (2016). Impacts of organic aerosols and its oxidation level on 698 CCN activity from measurement at a suburban site in China. Atmospheric Chemistry and 699 Physics 16 (8):5413–5425. doi:10.5194/acp-16-5413-2016.

701 TOC GRAPHIC

